Spin-disorder-induced Raman scattering from phonons in europium chalcogenides. I. Experiment

G. Güntherodt, R. Merlin,* and P. Grünberg†
Max-Planck-Institut für Festkörperforschung, 7 Stuttgart 80, Federal Republic of Germany
(Received 29 January 1979)

The symmetry-forbidden first-order Raman scattering in the paramagnetic phase of europium chalcogenides has been analyzed in terms of the Raman tensor components, their resonance enhancement, and the phonons involved. The most dominant scattering contribution is due to the antisymmetric Γ_{15}^{+} Raman tensor component. On the basis of the phenomenological theory of spin-dependent Raman scattering from phonons, the Γ_{15}^{+} component is a direct proof of simultaneous one-phonon one-spin excitations. Less intense but more resonantly enhanced contributions from the symmetric Γ_{12}^{+} and Γ_{25}^{+} components are due to one-phonon two-spin excitations. The anion-mass-dependent peak position of the first-order Raman scattering in the paramagnetic phase has been attributed to a locally full symmetric ($4f$) hole-phonon coupling, involving zone-boundary optic phonons. The associated breakdown in $\vec{k}$-selection rule originates from the disorder of the spin system in the paramagnetic phase. A proposed model for the scattering process under optical $4f^7 \rightarrow 4f^6 5d^1$ excitation predicts a transition from one-phonon zero-frequency spin excitations in the paramagnetic phase to one-phonon one-magnon excitations in the magnetically ordered phase, consistent with our experimental observations.

I. INTRODUCTION

In the study of inelastic light scattering of magnetic semiconductors the effect of magnetic order on Raman scattering (RS) from phonons has attracted considerable attention in recent years.[1] The investigations have been concentrated mainly on the chromium-chalcogenide spinels[2–6] and the europium monochalcogenides EuX (X = O,S,Se,Te).[1,7–27] For fixed exciting laser frequency in the Cr-chalcogenide spinels the magnetic order affects the phonon RS intensity through "resonance tuning" of the interband transitions undergoing exchange splittings upon cooling below the Curie temperature.[4–6] On the other hand, in the EuX compounds, with the localized, magnetic $4f$ states as initial states in the RS process, a simultaneous excitation of the spin and phonon systems via spin-orbit coupling in the excited, intermediate state has been revealed recently.[20] Similar conclusions have been arrived at in a model by Sakai and Tachiki.[24] A phenomenological treatment of this problem has been presented by Safran *et al.*[22,25]

In this paper we are concerned with spin-dependent RS of EuX, the most simple, model-type class of magnetic semiconductors which crystallizes in the NaCl structure.[16] Although first-order phonon RS of EuX is forbidden because of inversion symmetry, it nevertheless shows some new, anomalous features, which seem to be unique to this class of magnetic semiconductors: In the paramagnetic phase of EuX an overtone sequence is observed at multiple frequencies of a fundamental ω_0.[8,10,16,17] The latter is positioned between the zone-center TO and LO phonon frequencies and is due to first-order phonon RS.[8,10,17] Hence the fundamental ω_0 appears to be symmetry forbidden. Tsang *et al.*[8] have proposed a symmetry-breaking mechanism for the first-order RS in the paramagnetic phase of EuX in terms of spin disorder. On the other hand, Vitins and Wachter[12,19,28] attributed the qualitatively similar appearance of multiphonon inelastic light scattering in magnetic ordering EuX and diamagnetic YbX (X = S,Se,Te) to a "hot luminescence" process, thus seemingly disproving the spin-disorder model for EuX. This model has been questioned[16,17,21] and discarded recently.[20,29] In focusing on the qualitatively similar appearances of multiphonon light scattering in EuX and YbX, Vitins and Wachter overlooked the quantitatively different phonons, selection rules, and magnetic ground states involved in the RS of EuX, particularly in the paramagnetic phase,[16,17,20] and of YbX at all temperatures.[16,29] In the latter case, as well as in ferromagnetically saturated EuX,[1,7,9,14,21] the first-order "forbidden" LO(Γ) scattering is understood in terms of finite wave-vector effects in the Raman tensor due to the Fröhlich electron-phonon interaction.[30]

In this paper the main emphasis is on *first-order* spin-dependent RS from phonons in the *paramagnetic* phase of EuX, where the scattering mechanism has been rather controversial until recently.[20,24,25,27] Previously, the evidence for spin-disorder-induced RS in the paramagnetic phase of EuX has been deduced mainly from the temperature- and magnetic-field-dependent quenching of the scattering intensity upon

cooling through the magnetic ordering temperature.[8,9] However, the experimental data, especially the symmetry analysis in the paramagnetic phase, were incomplete. Hence, in the model of spin-dependent phonon RS of EuS by Suzuki,[13] the mechanism of simultaneously exciting the phonon and spin systems, involving spin-orbit coupling and the antisymmetric Raman tensor component, has been omitted. On the other hand, the model of spin-disorder RS by Safran *et al.*[22] arrives for the one-phonon one-spin mechanism at a symmetric Raman tensor, which disagrees with our experimental and theoretical findings[20] and also with the model by Sakai *et al.*[24]

Our measurements of the polarization dependence and resonance enhancement of the symmetry-forbidden first-order phonon RS of EuS and EuSe at 300 K around the fundamental gap have revealed the dominant contribution of the antisymmetric Γ_{15}^{+} Raman tensor component. This fact has provided the basis for the explanation of the frequency position and line shape of the scattered spectra in terms of a parameter-free microscopic theory. The model considers the simultaneous excitation of the phonon and spin systems, the spin-orbit coupling of the $4f$ electrons in the excited, intermediate state, and a locally full symmetric coupling of the localized $4f$ hole to LO phonons. The uncorrelated Eu^{2+} ion spins in the paramagnetic phase are taken into account by the incoherent part of the spin-correlation function, entering the RS cross section.

Our work has been divided into two parts: an experimental (I) and a theoretical (II)[31] part. Section II of the experimental part (this paper) deals with our experimental results on RS in the paramagnetic phase, including the effect of diluting the Eu ions and of the magnetic order on this scattering. The experimental results are discussed in Sec. III in terms of the phenomenological theory of spin-dependent RS. The microscopic theory is introduced in Sec. II of the theoretical part[31] which is the basis for the calculation of the RS cross section for the paramagnetic phase (see Sec. III of Paper II). Section IV of the theoretical part is concerned with the lattice-dynamical model for calculating the phonon dispersion curves and the Raman spectra.

II. EXPERIMENTAL RESULTS

A. Sample preparation and experimental technique

The preparation technique for single crystals of EuX and $Eu_{1-x}Gd_xS$ used in this work has been taken from the literature.[32] Handling of the materials has been performed in an argon box. The molybdenum and tungsten crucibles used for the crystal growth have been sealed in vacuum by electron beam welding. The EuO samples have been prepared from an Eu_2O_3–Eu mixture, with the Eu_2O_3 pressed into pellets and heated in vacuum. EuS single crystals have been prepared either from the elements or from powder produced by the H_2S reduction of Eu_2O_3. Metallographic investigations have revealed that the EuS single crystals grown from the elements showed less or no precipitates compared to the crystals grown from the prereacted powder. The Eu ^{34}S single crystals (90% enrichment of ^{34}S) have been grown in a tungsten crucible from material prereacted from the elements. The crystals showed no precipitates. Single crystals of $Eu_{1-x}Gd_xS$ have been grown by sealing the elements in the appropriate ratio into tungsten crucibles. The material with 10 at.% Gd showed very few, homogeneously distributed precipitates in the ingot, increasing in density and size towards the crystal-gas interface. Polycrystalline films of $Eu_{1-x}Gd_xS$ ($x=0.09, 0.30$) have been prepared by simultaneous evaporation of pressed EuS powder and GdS crystals in ultrahigh vacuum.[33] (RS on films with $x=1.0$ has been reported elsewhere.[34]) EuS has been evaporated from a tungsten crucible by electron beam bombardment, whereas GdS has been evaporated by current heating of a tungsten boat. The glass substrates have been heated to 320 °C. The pressure during evaporation rose from about 5×10^{-9} Torr to about 10^{-5} Torr. The deposition rates of GdS ($\leq$6 Å/ sec) and of EuS (15 Å/ sec) have been controlled by two quartz oscillator systems. After deposition, the films have been annealed for 1 h at 350 °C and 10^{-8} Torr. The NaCl stucture of the $Eu_{1-x}Gd_xS$ films has been confirmed by transmission-electron microscopy of samples evaporated onto small carbon films, which have been evaporated simultaneously with the glass substrates. The composition of the films has been determined by x-ray fluorescence analysis.

Powders of the solid-solution system $Eu_{1-x}Sr_xS$ have been prepared by Pink of Siemens Research Laboratory, Munich, using a method described elsewhere.[35]

The RS spectra presented in this paper have been measured by conventional technique, such as double monochromator with holographic grating and photon counting. Special care has been taken to keep sample heating by the laser light as low as possible. For the measurements at low temperatures the samples have been either kept in He exchange gas or immersed into pumped liquid He. The samples used in our investigations have been always freshly cleaved prior to the measurements.

B. First-order RS in the paramagnetic phase

Resonant RS of EuX is restricted to the first absorption maximum between 1 and 3.5 eV,[36] using the

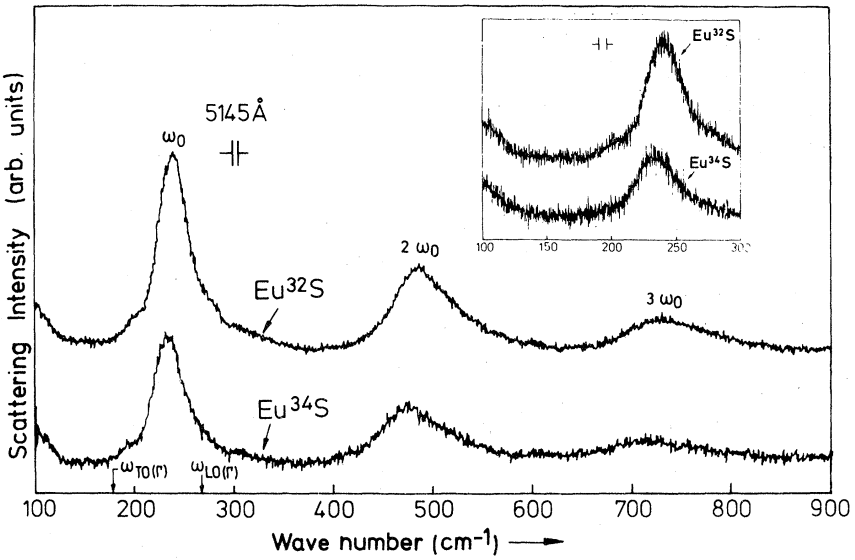

FIG. 1. Raman spectrum (unpolarized) of EuS at 300 K for two different S isotopes.

commercially available gas lasers and photon counting techniques. This absorption maximum has been assigned on experimental grounds to a $4f^7 \rightarrow 4f^6 5d(t_{2g})$ transition, i.e., from the localized $4f$ level into the lower crystal-field split $5d$ state.[36] RS of EuO has escaped experimental observation for a long time. As we have reported earlier[17] the Raman spectrum of EuO at 300 K shows a fundamental ω_0 and subsequent overtones. The fundamental at $\omega_0 = 411$ cm^{-1}, with a half-width of 100 cm^{-1}, is positioned between the zone-center TO (182 cm^{-1}) and LO (435 cm^{-1}) phonon frequencies.[37] This is consistent with the findings for all other EuX compounds in their paramagnetic phase.[8,12,16] The salient features of RS of EuO have been found to be practically independent of different quality and stoichiometry of the samples. However, a strong Stokes as well as anti-Stokes luminescence is easily encountered which most likely has obscured the proper observation of RS of EuO in previous attempts.[7,8,12,28] This luminescence has been investigated and attributed to the presence of Eu^{3+} impurities.[39]

In order to gain direct information about the phonons contributing to the fundamental ω_0 of EuX in the paramagnetic phase, we have substituted anions as well as cations (see Sec. II E). In the case of EuS we have chosen two different S isotopes, ^{32}S and ^{34}S. Figure 1 shows the Raman spectra of Eu ^{32}S and Eu ^{34}S at 300 K. The spectrum of Eu ^{32}S shows the well-known features, consisting of a fundamental at $\omega_0 = 240$ cm^{-1} and its higher harmonics.[8,10] The fundamental ω_0 with 30 cm^{-1} half-width is positioned between the zone-center phonon frequencies $\omega_{TO} = 178$ cm^{-1} and $\omega_{LO} = 267$ cm^{-1}.[38] Substituting ^{32}S by the ^{34}S isotope results in a 5 cm^{-1} shift of the fundamental ω_0 from 240 to 235 cm^{-1} as shown in Fig. 1 (see inset). The higher harmonics are also subject to a shift by about twice the amount of the fundamental. The shifted frequency ω_0' of the fundamental ω_0 results directly from the anion mass ratio $\omega_0' = \omega_0 (M_{32_S}/M_{34_S})^{1/2}$. This is indicative of an anion mass dependence of the fundamental ω_0 in the paramagnetic phase of EuX.

The first order RS of EuSe and EuTe, respectively, is shown in Figs. 11 and 13 of Paper II. In going from EuO to EuTe the peak position ω_0 of the first-order RS shifts systematically towards lower frequencies and the half-width decreases from 100 cm^{-1} for EuO to 22 cm^{-1} for EuTe.

The above indication of an anion mass dependence of the frequency position of the fundamental ω_0 has been further tested for the whole EuX series at 300 K. The result is shown in Fig. 2, where the frequency of

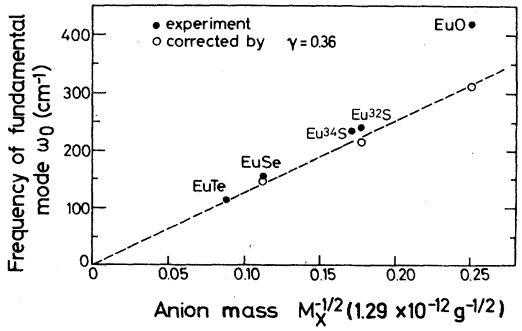

FIG. 2. Anion mass dependence of the peak position of first-order RS of EuX at 300 K; γ is the mode Grüneisen parameter [Eq. (1)].

the fundamental ω_0 of EuX at 300 K has been plotted versus the inverse of the square root of the anion mass $(M_X)^{-1/2}$. The full circles represent the experimental values. Except for EuO, the experimental points fall almost on a straight line through the origin. However, one also has to take into account the volume changes among the members of the EuX series. Thus we have corrected the values of ω_0 by a Grüneisen-like parameter

$$\gamma_{\vec{q},j} = -\frac{d[\ln \Omega_j(\vec{q})]}{d(\ln V)} , \quad (1)$$

where $\Omega_j(\vec{q})$ is the frequency of the phonon with wave vector $\vec{q}$ and branch index j, and V is the unit volume. Choosing V of EuTe as a reference, the whole EuX series has been fitted by a single, constant value of $\gamma = 0.36$, such that the corrected values of ω_0 (open circles in Fig. 2) fall on a straight line through the origin. Hence we conclude that the frequency of the fundamental ω_0 of EuX in the paramagnetic phase depends directly on the anion mass. The relationship established in Fig. 2 provides clear evidence that the dominant contribution to the fundamental ω_0 is from optic phonons at the zone boundary, with the lighter anions vibrating with respect to the heavier cations. Hence, another conclusion can be drawn that the fundamental ω_0 of EuX in the paramagnetic phase is due to first-order RS and does not result from a second-order process, like two acoustic phonons or one acoustic and one optic phonon. At first glance, this result seems to contradict $\vec{k}$ conservation. However, as will be shown below, the simultaneous excitation of the phonon and spin systems in the spin-disordered paramagnetic phase provides the additional degree of freedom to couple to phonon $\vec{q}$ vectors from the whole Brillouin zone (BZ).

C. Selection rules and resonance enhancement of first-order RS in the paramagnetic phase

The polarization dependence of the first-order RS of EuX in the paramagnetic phase has not been investigated systematically until recently.[20] Tsang *et al.*[8] did not find any polarization dependence in EuS and EuSe for exciting laser frequencies between 2.4 and 2.6 eV. On the other hand, Schlegel *et al.*[10] reported that for 2.81-eV laser excitation in EuS the polarization of 80% of the scattering intensity is rotated by 90° with respect to the incident polarization. In order to reconcile these two observations we have investigated the polarization dependence of the fundamental ω_0 of EuX at 300 K as a function of exciting laser frequency and for different scattering configurations.

In a first attempt we have analyzed the fundamental ω_0, i.e., first-order RS of EuS at 300 K with respect to the three irreducible, symmetric components of the Raman tensor for the O_h point group,[40,41] using (100), (110), and (111) single-crystal faces and linear polarized light. The evaluation of the Γ_1^+, Γ_{12}^+, and Γ_{25}^+ symmetry components from the integrated, absolute scattering intensities, however, revealed some inconsistencies. These could be resolved by implying that the antisymmetric Γ_{15}^+ component is nonzero. By using linear polarized light there are only three linearly independent equations for the four unknowns. However, if one considers that the contribution from each symmetry component $\Gamma_i^+ \geq 0$, we arrive at inequalities stating that $\Gamma_{15}^+ \neq 0$.

For a direct determination of the four independent symmetry components of the Raman tensor we used

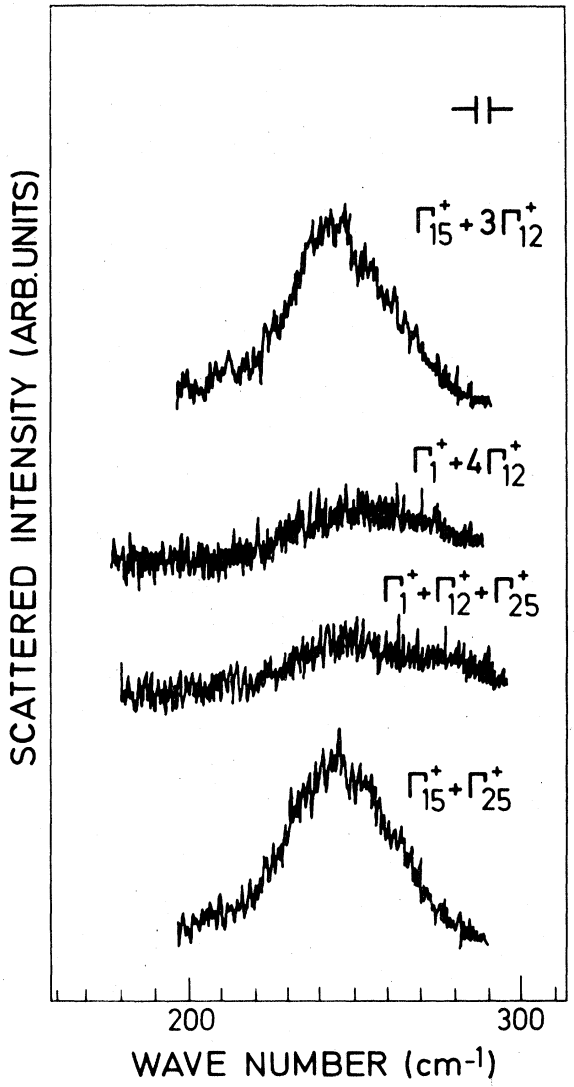

FIG. 3. Symmetry analysis of the Raman tensor of first-order RS from a (001) face of EuS at 300 K for 4416-Å laser excitation, using linearly and circularly polarized light.

in addition circular polarized light. Figure 3 shows the Raman spectrum for 4416-Å laser excitation of a cleaved (001) crystal face of EuS at 300 K. The following four different scattering geometries have been used (Fig. 3 from top to bottom): $z(x+y,x-y)\bar{z}$, $z(x,x)\bar{z}$, $z(x+iy,x+iy)\bar{z}$, and $z(x,y)\bar{z}$. The corresponding symmetry components for each of these scattering configurations are given in Fig. 3. By measuring the areas under the peaks one arrives at a system of four linearly independent equations, from which each irreducible symmetry component of the Raman tensor can be determined. Obviously there results that $\Gamma_{15}^{+} \neq 0$ and that it gives the most dominant contribution. This result confirms the earlier observation by Schlegel *et al.*[10] that the scattered light is polarized to 80% perpendicular to the incident polarization. However, they attributed the scattering to a dominant $T_{2g}(\Gamma_{25}^{+})$ component, whereas our analysis shows that it is due to the off-diagonal, but antisymmetric Γ_{15}^{+} component. The observation of the antisymmetric Raman tensor component is a surprising fact, since it is usually too small to be detected in RS from phonons.[41–43] The result analogous to Fig. 3 for 5145-Å laser excitation has been published earlier.[20]

Figure 4 shows the resonance enhancement of the Γ_{15}^{+} and the Γ_{12}^{+}, Γ_{25}^{+} scattering components of EuS at 300 K measured as a function of the exciting laser frequency between 1.5 and 2.8 eV. The Γ_{1}^{+} component has been found to be zero within experimental errors. The scattering intensities have been corrected for the absorption, measured on the very same sample used for the resonant RS experiment and also taken from the literature.[36] Moreover, particular care has been taken for the corrections involved in the experiment, i.e., different responses of the circular and linear polarizers, spectrometer response, and background subtraction. The largest errors arose in determining the areas under the peaks as indicated by the error bars in Fig. 4. Over the frequency range used, the dominant contribution to the first-order RS in the paramagnetic phase results from the antisymmetric Γ_{15}^{+} Raman tensor component. The resonance enhancement is over more than two orders of magnitude. On the other hand, the Γ_{12}^{+} and Γ_{25}^{+} components are, compared to the Γ_{15}^{+} component, weaker in intensity, but more resonantly enhanced, i.e., appear in a narrower energy region. Analogous results for EuSe are shown in Fig. 5. In this case we had difficulties in measuring the resonance enhancement in the vicinity of the fundamental gap because of the occurrence of the Franck–Condon luminescence. With respect to the relative intensities of the different scattering components the behavior of EuSe is very similar to that of EuS. The solid and dashed lines in Figs. 4 and 5 are the results of the microscopic theory, which will be presented in Paper II, Sec. III. In the case of EuSe the agreement between experiment and theory is worse compared to EuS.

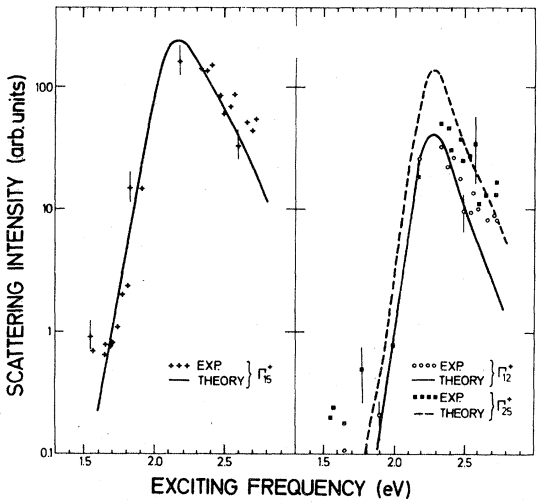

FIG. 4. Resonance enhancement of first-order RS of EuS at 300 K for the antisymmetric (Γ_{15}^{+}) and symmetric (Γ_{12}^{+}, Γ_{25}^{+}) Raman tensor components; the full symmetric (Γ_{1}^{+}) component is zero within experimental errors. The solid and dashed lines are the result of the microscopic theory in Paper II (Ref. 31).

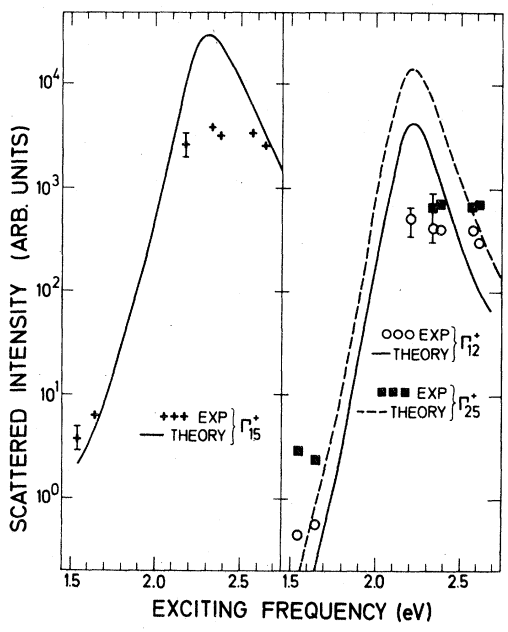

FIG. 5. Resonance enhancement of first-order RS of EuSe at 300 K for the antisymmetric (Γ_{15}^{+}) and symmetric (Γ_{12}^{+}, Γ_{25}^{+}) Raman tensor components,; the full symmetric (Γ_{1}^{+}) component is zero within experimental errors. The solid and dashed lines are the result of the microscopic theory in Paper II (Ref. 31).

This is mainly due to systematical experimental errors because of the subtraction of the luminescence background.

D. Effect of magnetic order on first-order RS

In order to fully elucidate the scattering mechanism of first-order RS in the paramagnetic phase of EuX, we have extended our investigations into the magnetically ordered phase. The effect of magnetic order on RS from phonons in EuX has been investigated in previous works quite extensively.[8–17,19,21–27] A temperature- and magnetic-field-dependent quenching of the scattering intensity of EuS and EuSe in the paramagnetic phase has been observed upon cooling below the ordering temperature.[8–10,12] The intensity quenching in the vicinity of the Curie temperature of EuS has been shown to follow a spin-correlation function.[10,11] On the other hand, for EuO as well as EuTe the scattering intensity has been reported to be independent of magnetic order.[12] The increase of the scattering intensity of the first-order RS in EuTe upon cooling below the Néel temperature has been considered by Vitins *et al.*[12,28] as evidence against the spin-disorder induced RS in the paramagnetic phase.

Here we report selected complementary data of the magnetic-order dependence of first-order RS in EuX, in support of the model of spin-disorder induced RS in the paramagnetic phase[20] and consistent with its extension into the magnetically ordered phase. In Fig. 1 of Ref. 26 we have shown the temperature dependence of the $\Gamma_{25}^{+}+\Gamma_{15}^{+}$ components of first-order RS of EuO for 5145-Å laser excitation. Upon cooling from 300 to 5 K the integrated scattering intensity does not follow the usual Bose factor.[34,42,44] The intensity decreases for 125 K, shows a weak maximum slightly above the Curie temperature $T_C=69$ K and quenches strongly below T_C. However, at 5 K we still observe a nonvanishing scattering intensity, which extends well beyond the estimated LO(Γ) phonon frequency of about 438 cm^{-1} at 5 K.[37] The peak position of the fundamental ω_0 shows a shift from 411 cm^{-1} at 300 K to about 445 cm^{-1} at 5 K which is unusually large for phonons only. Similar temperature dependences of the peak position and integrated peak intensity of the fundamental ω_0 have also been observed in EuS. In Fig. 6 we show the temperature dependence of the peak position of the fundamental ω_0 of EuO and EuS for 5145-Å laser excitation. The shift of ω_0 upon cooling from room temperature in both cases deviates from the expected linear behavior at temperatures slightly above the Curie temperature T_C. The total frequency shift from 300 to 4.2 K of $\Delta\omega_0/\omega_0=17\%$ in EuO and $\Delta\omega_0/\omega_0=25\%$ in EuS is much larger that what is expected from the temperature variation of the lattice constant, including also the magnetostrictive contribution below T_C. The total change in lattice constant between 300 and 4.2 K is $\Delta a_0/a_0=0.33\%$ for EuO and $\Delta a_0/a_0=0.28\%$ for EuS.[45] According to the relation

$$\Delta\omega/\omega=-3\gamma\Delta a/a \tag{2}$$

and using $\gamma=0.36$ from Fig. 2, we obtain total frequency shifts of $\Delta\omega/\omega=0.36\%$ for EuO and $\Delta\omega/\omega=0.31\%$ for EuS between 300 and 4.2 K. Hence we conclude that the nonlinear temperature-dependent shift of ω_0 has to be attributed to the onset of magnetic order, but is not associated with magnetostriction. The onset of this nonlinear shift for $T\gtrsim T_C$ is most likely due to the onset of magnetic short-range order. In particular, we would like to point out that the magnetic-order-induced shift of ω_0 has nothing to do with a resonance effect associated with the excited, intermediate state undergoing an exchange splitting for $T\lesssim T_C$. The 5145-Å (2.41-eV) laser excitation used in Fig. 6 falls in the case of EuO into a region where the optical $4f^7\rightarrow 4f^6 5d(t_{2g})$ transitions do not show any shifts as seen in the magneto-optical spectra.[36,46,47] Thus the shift ω_0 in Fig. 6 cannot be attributed to the emergence of the "forbidden" LO(Γ) scattering as claimed by Safran.[25] This scattering should show a strong and fairly sharp resonance near $E_1''=1.55$ eV.[14,21,45] The above considerations are also contrary to our previous interpretation[17] that ω_0 shifts at very low temperature to the frequency of the LO(Γ) phonon.

On the other hand, the case of the antiferromagnet EuTe has been shown in Fig. 2 of Ref. 26 for temperatures above and below the Néel temperature $T_N=9.8$ K and for resonant 5145-Å laser excitation. No shift of the peak position ω_0 is observed in the $\Gamma_1^{+}+4\Gamma_{12}^{+}$ scattering configuration upon cooling from

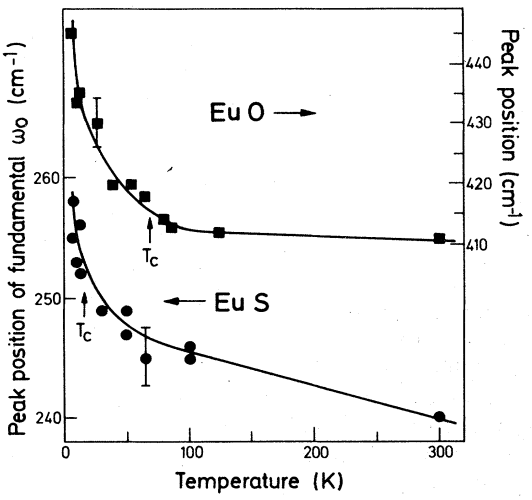

FIG. 6. Temperature dependence of the peak positions ω_0 of first-order RS ($\Gamma_{25}^{+}+\Gamma_{15}^{+}$) of EuO and EuS for 5145-Å laser excitation.

300 to 2 K. A small shift of 3 cm^{-1} is observed for the $\Gamma_{25}^{+}+\Gamma_{15}^{+}$ Raman tensor components. Contrary to the ferromagnets EuO and EuS, antiferromagnetic EuTe shows an increase in the first-order RS intensity for $T < T_N$. In the scattering intensity at 2 K the $\Gamma_1^+ + 4\Gamma_{12}^+$ symmetry components dominate over the $\Gamma_{25}^{+}+\Gamma_{15}^{+}$ components.

E. Single-ion effects

We have also performed RS measurements on solid-solution systems obtained by substituting Eu^{2+} by isoelectric Sr^{2+} or Gd^{3+} ions. The dilution of the Eu^{2+} ions in such solid-solution systems provides a good test of the scattering mechanism and the spin correlations involved in the various magnetic phases.

In Fig. 7 we show the Raman spectrum of a (100) single-crystal face of $Eu_{0.67}Sr_{0.33}O$ at 300 K. This spectrum is very similar to that of Fig. 1 in Ref. 17. In particular, the frequency positions $n\omega_0 (n = 1, 2, 3, \ldots)$ of EuO are unchanged upon Sr substitution, in agreement with the anion mass dependence of ω_0 in Fig. 2. For the fundamental ω_0 the dominant contribution to the scattering intensity is from the $\Gamma_{25}^{+}+\Gamma_{15}^{+}$ symmetry components. This is qualitatively consistent with the findings for EuS and EuSe in Sec. II C.

The Raman spectra of the $Eu_{1-x}Sr_xS$ solid-solution system at 300 K are shown for $x = 0.05$, 0.6, and 0.9 in Fig. 8. Because of the powder samples used in these measurements, the quality of the spectrum of, e.g., $Eu_{0.95}Sr_{0.05}S$ is poor compared to that of EuS in Fig. 1. However, we can again identify the unchanged frequency positions of the fundamental ω_0 and its overtones with varying x between 0 and 1.

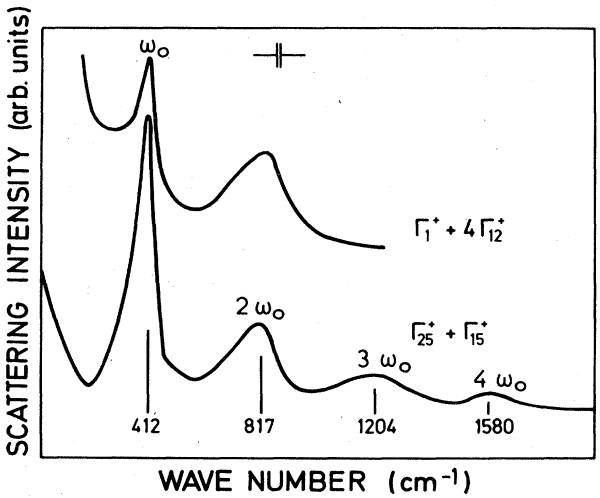

FIG. 7. Raman spectrum of a (100) single-crystal face of $Eu_{0.67}Sr_{0.33}O$ at 300 K for 5145-Å laser excitation (the scale of the Raman shift is linear in Å).

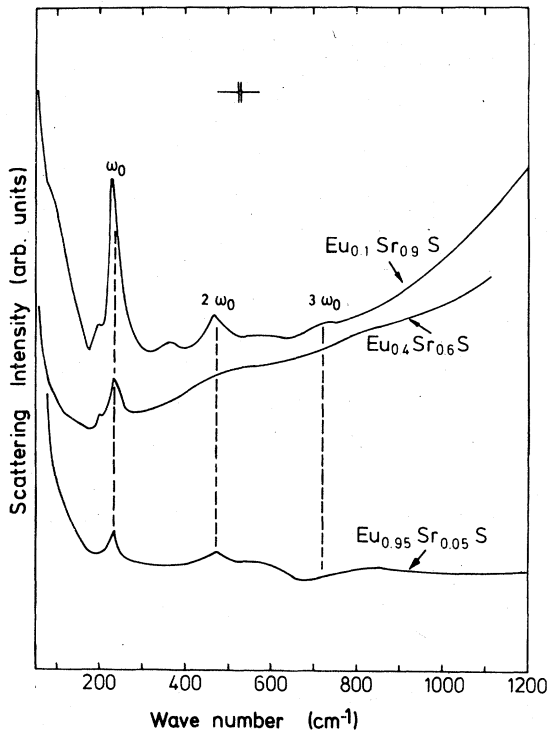

FIG. 8. Unpolarized Raman spectra of powder samples of the $Eu_{1-x}Sr_xS$ solid-solution system for $x = 0.05$, 0.6, and 0.9 at 300 K using 4579-Å laser excitation.

The rising background at higher Stokes shifts for $x = 0.6$ and $x = 0.9$ in Fig. 8 is attributed to the onset of the Franck–Condon luminescence. EuS shows a luminescence below 150 K with a Franck–Condon shift of 0.5 eV.[48] With increasing x in $Eu_{1-x}Sr_xS$, however, the Franck–Condon shift decreases and the emission intensity becomes increasingly strong at room temperature.[49]

In the $Eu_{1-x}Sr_xO$ and $Eu_{1-x}Sr_xS$ solid-solution systems the ionic radii of Sr^{2+} (1.13 Å) and Eu^{2+} (1.12 Å) are very similar, whereas their masses differ significantly. The unchanged frequency positions of the fundamental ω_0 and its overtones upon substituting Eu^{2+} by Sr^{2+} are in further support of an anion mass dependence of ω_0 as concluded from Fig. 2.

That the RS of EuX in the paramagnetic phase is indeed associated with a single-ion effect has been tested in the case of $Eu_{0.1}Sr_{0.9}S$. This material shows a spin-glass behavior,[50] i.e., the Eu^{2+} ion spins are statistically distributed over the lattice sites without any long-range order between them. On the other hand, the spin disorder in EuS for $T >> T_C$ refers to the thermally disordered orientations of the Eu^{2+} ion spins whose distribution otherwise has the periodicity of the lattice. Figure 9 clearly demonstrates that the scattering intensity and the frequency position of the

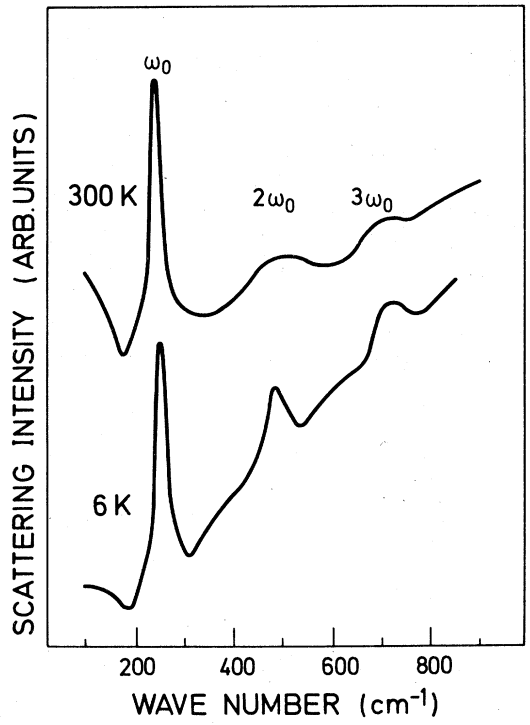

FIG. 9. Temperature dependence of the unpolarized Raman spectrum of $Eu_{0.1}Sr_{0.9}S$ (powder) for 4579-Å laser excitation.

fundamental ω_0 at 300 K do not change significantly upon cooling to 6 K. This is contrary to the magnetic-order-induced quenching of the scattering intensity and the shift in peak position of the fundamental ω_0 of EuO and EuS in Fig. 6. Also the overtones ($2\omega_0$ and $3\omega_0$) do not shift in frequency upon cooling, but become rather slightly more pronounced. The result of Fig. 9 provides clear evidence that the first-order RS in the paramagnetic phase of EuX is due to uncorrelated single Eu^{2+} ion spins.

Practically unchanged frequency positions $n\omega_0(n=1,2,\ldots)$ of EuS are also found in the $Eu_{1-x}Gd_xS$ solid-solution system. In Fig. 10 we show Raman spectra of thin films with $x=0.09$ and $x=0.3$ at 300 K. However, with respect to the scattering intensities the $Eu_{1-x}Gd_xS$ system behaves differently with increasing x compared to $Eu_{1-x}Sr_xS$ in Fig. 8. In going from $x=0.09$ to $x=0.3$ in Fig. 10 the intensity of the ω_0 and $2\omega_0$ peaks is strongly quenched. For $x=0.09$ also the ratio of integrated intensities $I_{2\omega_0}/I_{\omega_0}$ is much smaller compared to that observed for the EuS in Fig. 1. The intensity quenching with increasing Gd concentration in $Eu_{1-x}Gd_xS$ cannot be due to the dilution of Eu^{2+} ions as is obvious from Fig. 8. The difference, however, between Sr^{2+} and Gd^{3+} substitutions in EuS is that each Gd^{3+} ion contributes one conduction electron and that the ionic radius of Gd^{3+} (1.02 Å) is by 9% smaller than that of Eu^{2+} and Sr^{2+}. An intensity quenching of the ω_0 and $2\omega_0$ peaks in Fig. 10 due to increasing free-carrier concentration with increasing Gd concentration is very unlikely. No change in the scattering intensity of the fundamental ω_0 has been found for insulating and conducting samples of EuS and EuSe at 300 K.[8] Our RS experiments of EuO_x, containing oxygen vacanies and undergoing a semiconductor-metal transition,[51] did also not reveal any free-carrier-induced intensity quenching at the phase transition. This is consistent with the conclusion in Sec. II B, that zone-boundary optic phonons are contributing to the fundamental ω_0 of EuX at 300 K. The latter phonons will not be subject to screening by free carriers as discussed for GdS.[34] Hence, an ionic size effect of the smaller Gd^{3+} ions, inducing a lattice distortion in the EuX matrix and influencing the electron-phonon coupling, might be responsible for the changes in scattering intensity with increasing x in $Eu_{1-x}Gd_xS$ (Fig. 10) and will be discussed in Sec. III.

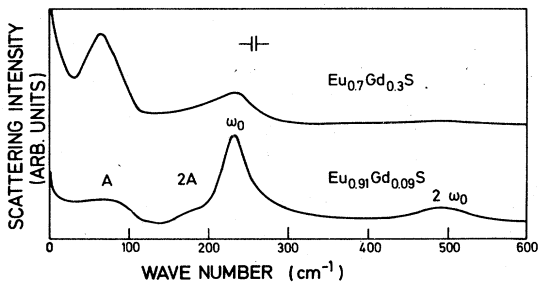

FIG. 10. Unpolarized Raman spectra of the $Eu_{1-x}Gd_xS$ solid-solution system for $x=0.09$ and 0.3 at 300 K using 5145-Å laser excitation. (Spectra for $x=1.0$ have been published in Ref. 35.)

The bands A and $2A$ at lower frequencies than ω_0 in Fig. 10 denote, respectively, first-order defect-induced and second-order RS from acoustic phonons. The first-order RS (A) for $x=0.09$ is found to increase strongly for $x=0.3$, i.e., upon introducing additional defects in the EuS lattice. This assignment is consistent with that for GdS.[34]

The role of lattice defects and spin correlations in the $Eu_{1-x}Gd_xS$ solid-solution system has been tested for a single crystal with $x=0.1$. The effect of the Gd dopant on EuS is to provide nominally one conduction electron per Gd^{3+} ion and to increase the Curie temperature from 16.5 K for $x=0$ to 50 K for $x=0.1$.[52] The Raman spectrum of $Eu_{0.9}Gd_{0.1}S$ at 300 K in Fig. 11 shows, like in Figs. 1 and 10, a fundamental ($\omega_0=240$ cm^{-1}) and its overtone. Cooling from 300 to 7 K results in a strong quenching of the fundamental ω_0 in Fig. 11 and in a shift of its peak position of similar magnitude as that of EuS in Fig. 6. At 7 K some residual structure is observed between

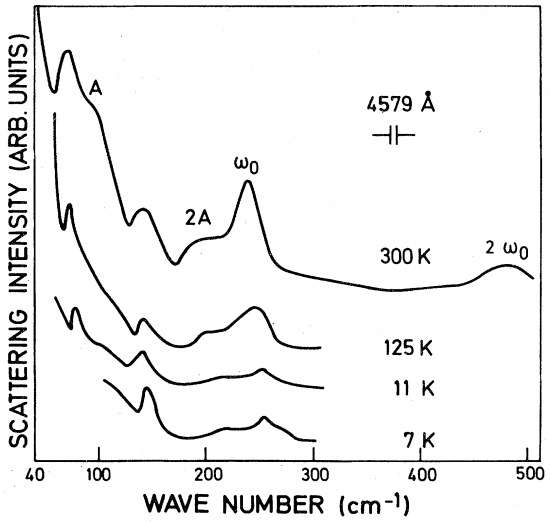

FIG. 11. Temperature dependence of the $\Gamma_{25}^{+}+\Gamma_{15}^{+}$ Raman spectrum of a (100) single-crystal face of $Eu_{0.9}Gd_{0.1}S$ for 4579-Å laser excitation.

200 and 280 cm^{-1}. In particular, a broad shoulder extends up to 280 cm^{-1}, i.e., beyond $\Omega_{LO}(q=0) \simeq 270$ cm^{-1}.

The broad bands below 130 cm^{-1} (A) and around 200 cm^{-1}($2A$) are very similar to those in Fig. 10. They are attributed to defect-induced first-order RS and allowed second-order RS from acoustic phonons, respectively. Both bands are reduced in intensity upon cooling, approximately in agreement with the Bose factor. The two peaks at 70 and 140 cm^{-1}, respectively, coincide roughly with the TA(L) and LA(L) phonon frequencies (see Paper II, Sec. II). They sharpen upon cooling and shift slightly towards higher frequencies. These two peaks can possibly be due to local modes associated with the Gd substituents, giving rise to acoustic modes. They have not been observed in Fig. 10 presumably because of the polycrystalline structure of the thin evaporated films.

F. Second-order RS

While the first-order RS from phonons in the NaCl structure is parity forbidden, the second-order RS from phonons is allowed. As a representative example we show in Fig. 12 (top) EuS for 7993-Å laser excitation, which is below the absorption edge of 7522 Å (1.65 eV).[36] The spectrum of the $\Gamma_1^+ + 4\Gamma_{12}^+$ scattering components is similar to the second-order Raman spectrum of SrO.[53] In particular, it shows also a cutoff around the 2LO(Γ) phonon frequency [534 cm^{-1} (Ref. 38)] and a broad maximum just below this frequency (~ 480 cm^{-1}) which has been attributed in both cases[17,53] to 2LO(L) phonons. An assignment has been given elsewhere[17] and a further

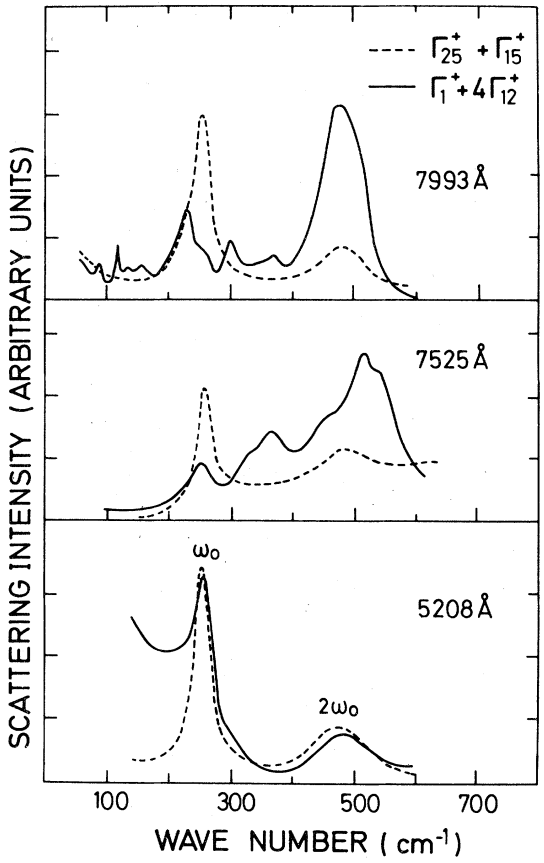

FIG. 12. $\Gamma_1^+ + 4\Gamma_{12}^+$ and $\Gamma_{25}^+ + \Gamma_{15}^+$ Raman spectra of EuS at 300 K for different laser excitations below (7993 Å), in the vicinity (7525 Å), and above (5208 Å) the fundamental absorption edge.

discussion in terms of the calculated two-phonon density of states will be given in Sec. IV of Paper II. The rich structure of the $\Gamma_1^+ + 4\Gamma_{12}^+$ scattering components changes in intensity and finally disappears as the exciting laser line approaches the maximum of the $4f^7 \rightarrow 4f^6 5d(t_{2g})$ absorption band around 5400 Å.[36] For 5208-Å laser excitation in Fig. 12 (bottom) the $\Gamma_1^+ + 4\Gamma_{12}^+$ and $\Gamma_{25}^+ + \Gamma_{15}^+$ spectra become very similar. Interestingly enough the $\Gamma_{25}^+ + \Gamma_{15}^+$ spectrum is practically the same for all three laser lines shown in Fig. 12. Thus the $n\omega_0$ overtone sequence of Fig. 1 is also observed for the 7993-Å laser excitation, which is by $3\omega_0$ *below* the fundamental gap. Obviously, this observation rules out a recombination process of "hot" electrons which has been suggested by Vitins and Wachter[12,19,28] as explanation for the multiphonon RS in EuX.

Figure 12 shows clearly that second-order RS in EuS is observed only for nonresonant laser excitation below or in the vicinity of the fundamental gap. On the other hand, for resonant $4f \rightarrow 5d$ excitation,

first-order RS and its iterated overtone processes dominate. Second-order RS of EuSe and EuTe, respectively, is shown in Figs. 8 and 10 of Paper II. We did not observe second-order RS in EuO because its fundamental gap is at 1.1 eV, i.e., in a spectral region which is not easily accessible.

III. DISCUSSION

A. First-order RS in the paramagnetic phase

RS of EuO has been reported previously to be of weak intensity[7,8,12] and even independent magnetic order.[12] Tsang *et al.*[8] attributed this weak scattering intensity to the nonresonant excitation by the laser lines used. On the other hand, in the "hot luminescence" model Vitins and Wachter[12,28] the apparently weak scattering intensity of EuO was assumed to result from a low probability of radiative recombination because of the large orbit of the excited electron.

Our previous results[17,26] and those in Figs. 2 and 6 clearly show that EuO behaves according to a systematic trend throughout the EuX series. In particular, EuO exhibits the largest number of overtones which decreases from EuO to EuTe.[16] This is consistent with earlier predictions by Tsang *et al.*[8] on the basis of the Williams-Smit model.[54]

Previously, several more qualitative arguments have been given in support of *first-order* RS for the fundamental ω_0 of EuX at 300 K.[8] A quantitative comparison of the Stokes to anti-Stokes scattering intensity ratio for the fundamental ω_0 of EuS, however, cannot distinguish between a first- or second-order process as claimed by Schlegel *et al.*[10] For $\omega_0 = 240$ cm^{-1} the ratios turn out to be the same for first- or second-order RS. Moreover, the temperature dependence of the integrated intensity of the fundamental ω_0 of EuO,[26] EuS (Sec. II D) and EuSe, EuTe (Ref.12) does not at all follow the Bose factor. Hence, no direct information can be obtained concerning first- or second-order RS. The above considerations emphasize the importance of the relationship established in Fig. 2 in order to identify the fundamental ω_0 in EuX as a one-phonon scattering process. This will be further corroborated by the microscopic description of the line shape of ω_0 by a weighted one-phonon density of states from the LO branch (see Paper II, Sec. IV).

B. Electron-phonon coupling

The result in Fig. 2 shows that optic phonons, mainly from the zone boundary, contribute to the fundamental ω_0 because of their high density of states (see Paper II, Sec. IV). In this section we discuss the electron-phonon coupling mechanism under optical $4f \rightarrow 5d$ excitation and the hence deduced phonon symmetries involved in the first-order RS of EuX in the paramagnetic phase.

In the EuX series the highest occupied electronic states are the localized $4f^7$ states of Eu^{2+}. They are initial states in RS for photon energies between 1 and 3 eV. With the optical excitation of $4f^7(Eu^{2+}) \rightarrow 4f^6 5d^1(Eu^{3+})$ there is associated a 14% reduction in ionic radius of Eu^{2+}.[55] The resulting isotropic compression couples to the locally full symmetric (Γ_1^+) displacements of the ions with respect to the Eu ion. Considering the nearest-neighbor (nn) approximation one can write the full symmetric combination of displacements of the six nn S ions as follows:

$$U_m^{\Gamma_1^+} = (u_{x,\vec{r}_1} - u_{x,-\vec{r}_1}) + (u_{y,\vec{r}_2} - u_{y,-\vec{r}_2}) + (u_{z,\vec{r}_3} - u_{z,-\vec{r}_3}) \quad , \tag{3}$$

with

$$\vec{r}_1 = \tfrac{1}{2}a(1,0,0), \quad \vec{r}_2 = \tfrac{1}{2}a(0,1,0), \quad \vec{r}_3 = \tfrac{1}{2}a(0,0,1) \quad ,$$

where $U_m^{\Gamma_1^+}$ is the combination of nn ion displacements of Γ_1^+ symmetry with respect to site $\vec{r}_m$, $u_{j\vec{r}_n}$ is the j component ($j = x,y,z$) of the displacement of the ion at site $\vec{r}_n$ ($n = 1,2,3$) and a is the next-nearest-neighbor (nnn) Eu-Eu distance. The Fourier transform of Eq. (3) gives

$$Q_m^{\Gamma_1^+} = \frac{1}{(NM_X)^{1/2}} \sum_{l\vec{q}} e^{-i\vec{q}\cdot\vec{r}_m} Q_{l\vec{q}}\, h(l,\vec{q}) \quad , \tag{4}$$

with

$$h(l,\vec{q}) = w_x(l,\vec{q}) \sin\tfrac{1}{2}q_x a + w_y(l,\vec{q}) \sin\tfrac{1}{2}q_y a + w_z(l,\vec{q}) \sin\tfrac{1}{2}q_z a \quad ,$$

where N is the number of unit cells, M_X is the anion mass, w_j is the j component of the polarization vector, and $Q_{l\vec{q}}$ is the normal coordinate of a phonon with wave vector $\vec{q}$ and branch index l. The function $h(l,\vec{q})$ is zero for $\vec{q} = (0,0,0)$ and has its maximum at the zone boundary for $\vec{q} = (\pi/a)(1,1,1)$. It follows that the dominant contribution in this locally full symmetric electron-phonon coupling is from LO phonons at the L point of the BZ. The normal mode coordinates of the LO(L) phonons are indicated by the arrows in Fig. 13. The anion planes (hatched triangles) are vibrating against each other, with the Eu planes at rest.

In the case of $Eu_{1-x}Gd_xS$ in Fig. 10 a possible explanation for the quenching of the scattering intensity with increasing x may be a reduced electron-phonon coupling. The smaller size Gd^{3+} ions can induce a lo-

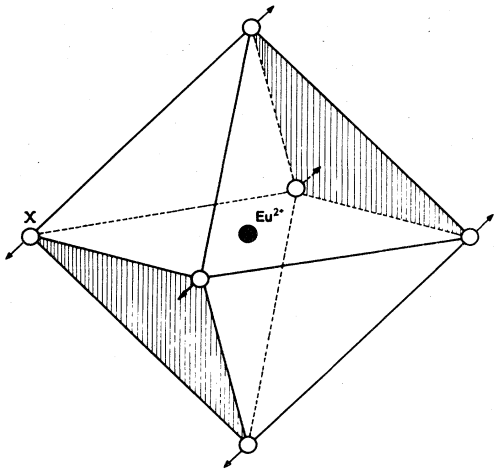

FIG. 13. Nearest-neighbor anion (X) coordination around a Eu^{2+} ion in the NaCl structure of EuX. The arrows indicate the normal mode coordinates of the LO(L) phonons.

cal lattice distortion in which the neighboring S ions will be closer to Gd^{3+} than to Eu^{2+}. This should manifest itself in a reduction of the strength of the full symmetric hole-phonon coupling. On the other hand, in the case of $Eu_xSr_{1-x}S$ the increase in scattering intensity with decreasing Eu concentration in Fig. 8 may be related to a resonant process. With decreasing x the $4f \rightarrow 5d$ transition shifts towards higher energy and overlaps increasingly with the laser line used.[56]

C. Spin-dependent RS in the paramagnetic phase

The most striking result of RS of EuX in the paramagnetic phase is the observation of the dominant antisymmetric Γ_{15}^+ scattering component in Figs. 3–5. In principle, the antisymmetric Raman tensor component should be observable in RS from phonons under resonance conditions, where the quasistatic approximation breaks down.[41,42,44] However, so far this has not been observed experimentally.[43] On the other hand, the antisymmetric Raman tensor component has been observed in light scattering from magnons[57] and electronic levels.[58] It has also been observed[59] and discussed[60] for vibronically active modes of electronic transitions. Since none of the above cases seem to apply to RS of EuX in the paramagnetic phase, and in view of the pronounced effect of magnetic order on first-order RS in EuX (Sec. II D), the observation of the antisymmetric scattering component has provided the basis for the model of spin-dependent RS in EuX. The microscopic description of this model will be presented in Sec. II of Paper II. Here we give an introduction based on the phenomenological theory.

In the phenomenological treatment of RS from phonons the electronic contribution to the susceptibility of the solid is expanded in powers of the displacements of the ions from their equilibrium positions. In spin-dependent RS from phonons the spin-dependent electric susceptibility is expanded in terms of the ion displacements and the ion spins.[3,13,24,61] Hence we have

$$\Delta\chi_{\alpha\beta}(\omega_i,u_{j\vec{r}_n},S_{\sigma\vec{r}_m}) = \sum_{j\vec{r}_n,\sigma\vec{r}_m}\frac{\partial^2\chi_{\alpha\beta}}{\partial u_{j\vec{r}_n}\partial S_{\sigma\vec{r}_m}}u_{j\vec{r}_n}S_{\sigma\vec{r}_m} + \sum_{j\vec{r}_n,\sigma\vec{r}_m,\sigma'\vec{r}'_m}\frac{\partial^3\chi_{\alpha\beta}}{\partial u_{j\vec{r}_n}\partial S_{\sigma\vec{r}_m}\partial S_{\sigma'\vec{r}'_m}}u_{j\vec{r}_n}S_{\sigma\vec{r}_m}S_{\sigma'\vec{r}'_m} + \cdots$$

$$= \sum R^{(2)}_{\alpha\beta j\vec{r}_n,\sigma\vec{r}_m}u_{j\vec{r}_n}S_{\sigma\vec{r}_m} + \sum R^{(3)}_{\alpha\beta,j\vec{r}_n,\sigma\vec{r}_m,\sigma'\vec{r}'_m}u_{j\vec{r}_n}S_{\sigma\vec{r}_m}S_{\sigma'\vec{r}'_m} + \cdots , \tag{5}$$

with $\chi_{\alpha\beta}$ as the frequency- , wave-vector-, and spin-dependent electric susceptibility tensor, ω_i as the incident laser frequency, $u_{j\vec{r}_n}$ as the j component of the displacement of the ion at site $\vec{r}_n$, $S_{\sigma\vec{r}_m}$ as the σ component of the ion spin at $\vec{r}_m$, and $\sigma,j=(x,y,z)$. $R^{(n)}_{\alpha\beta,j,\sigma}$ denotes the Raman tensor, with n accounting for the order of the derivatives of $\chi_{\alpha\beta}$ with respect to ion displacements and spins. Equation (5) describes RS under the simultaneous excitation of the phonon and spin systems. The first term of Eq. (5) is linear in the spin $\vec{S}$, which transforms like an axial vector according to Γ_{15}^+ in the point group O_h. This fact coupled with time-reversal invariance leads us to conclude that the Raman tensor $R^{(2)}_{\alpha\beta,j,\sigma}$ has to be *antisymmetric* (Γ_{15}^+ symmetry). The Raman-active phonon modes transform with respect to $\vec{r}_m$ as

$$\Gamma(u_{j\vec{r}_n}) = \Gamma_{15}^+ \otimes \Gamma_{15}^+ = \Gamma_1^+ \oplus \Gamma_{12}^+ \oplus \Gamma_{25}^+ \ .$$

According to our discussion of the electron-phonon coupling in Sec. III C only the Γ_1^+-symmetry phonons should be of importance.

On the other hand, the square of the spins in the second term of Eq. (3) is even under time reversal

$$\Gamma_{15}^+ \otimes \Gamma_{15}^+ = \Gamma_1^+ + \Gamma_{12}^+ + \Gamma_{25}^+ \ .$$

The full symmetric (Γ_1^+) component of the product of

the spin operators which transforms like S_σ^2, however, vanishes because it does not induce transitions in the spin system. Hence the Raman tensor $R^{(3)}_{\alpha\beta,j,\sigma,\sigma'}$ is symmetric and transforms like Γ_{12}^+ and Γ_{25}^+.

The above phenomenological symmetry analysis can account for our observations in Figs. 4 and 5. The dominance of the Γ_{15}^+ component is due to the one-phonon one-spin term in Eq. (5). On the other hand, the less intense contributions form the Γ_{12}^+ and Γ_{25}^+ components can be attributed to the one-phonon two-spin term in Eq.(5). This is consistent with the higher order of this term in the expansion of $\chi_{\alpha\beta}$ and with the more resonant enhancement due to the higher-order derivative of $\chi_{\alpha\beta}$. Moreover, the symmetry analysis is also consistent with our experimental findings in Figs. 3–5 that the Γ_1^+ component is zero within experimental errors.

The absence of spin-orbit coupling in the $4f^7(^8S_{7/2})$ ground state of Eu^{2+} excludes a direct spin-phonon interaction. Hence the spin and phonon systems are decoupled in the ground state and we can factorize the phonon- and spin-correlation functions in the Raman scattering cross sections. For the one-phonon one-spin term of Eq. (5) we can write

$$\frac{\partial^2\sigma}{\partial\Theta\partial\Omega}=\frac{\omega_i^4}{2\pi c^3}\sum_{\alpha\beta\alpha'\beta'}E^s_{\alpha'}E^s_{\beta'}E^i_\beta E^i_\alpha\frac{1}{2\pi}\int_{-\infty}^{+\infty}dt\,e^{-i\Omega t}\langle\chi_{\beta'\alpha'}(t)\chi^*_{\alpha'\beta}(0)\rangle$$

$$=\frac{\omega_i^4}{2\pi c^3}\sum_{\substack{\alpha\beta\alpha'\beta'\\ jr_n,\sigma r_m,\sigma' r_m'}}E^s_{\beta'}R^{(2)}_{j\alpha}E^i_\alpha E^s_{\alpha'}R^{(2)}_{j\alpha'\beta}E^i_\beta\,\frac{1}{2\pi}\int_{-\infty}^{+\infty}dt\,e^{-i\Omega t}\langle u_{j\vec{r}_n}(t)u^*_{j,-\vec{r}_n}(0)\rangle\,\langle S_{\sigma\vec{r}_m}(t)S^*_{\sigma'\vec{r}_m'}(0)\rangle\ , \tag{6}$$

where $E^{i(s)}_{\alpha(\alpha')}$ are the α (α') polarization-vector components of the incident (scattered) photon, $\Omega=\omega_i-\omega_s$ is the difference between the incident and scattered photon frequencies and $\langle\ \rangle$ is a thermal average. The last two terms in the angular brackets of Eq. (6) denote the phonon and the two-spin correlation functions. The former term contains the phonon normal coordinates, the phonon frequencies, and the Bose factor. A microscopic description of the scattered spectra has to account for three factors: (i) The coupling constants entering $R^{(2)}_{\alpha\beta}$, (ii) the electron-phonon coupling in form of phonon normal coordinates and their polarization vectors, and (iii) the spin-correlation function for the appropriate magnetic phase.

The spin-correlation function in Eq. (6) can generally be written[25,62]

$$\chi_{\sigma\sigma'}(\omega,\vec{q})=\sigma_{\sigma\sigma'}\delta(\omega-\Omega_j(\vec{q}))\,\langle S_\sigma(-\vec{q})\rangle\,\langle S_{\sigma'}(\vec{q})\rangle+\delta(\omega-\Omega_j(\vec{q})-\Omega_m(-\vec{q}))$$

$$\times\frac{1}{2\pi}\int_{-\infty}^{+\infty}dt\,e^{i\omega t}\langle S^*_\sigma(-\vec{q},0)S_{\sigma'}(\vec{q},t)\rangle\ , \tag{7}$$

where $S_\sigma(\vec{q})$ is the Fourier transform of the σ component of the spin in $\vec{q}$ space, $\omega=\omega_i-\omega_s$, $\Omega_m(\vec{q})$ is the frequency of a magnetic excitation with wave vector $\vec{q}$, and $\Omega_j(\vec{q})$ is that of the phonon with branch index j. The latter enters through the phonon-correlation function after transforming the ion displacements to phonon normal coordinates. The first term in Eq. (7) describes with respect to the spin system *coherent, elastic* scattering due to the average magnetization (sublattice magnetization) of a ferromagnet (antiferromagnet). Transitions in the spin system are neglected. Thus, if the magnetization is directed in z direction the elastic scattering is proportional to the square of the magnetization $\langle S_z\rangle^2$. The second term of Eq. (7) describes *inelastic* scattering due to magnetic short-range order. For $T<T_{C,N}$ this term describes magnon excitations.[62]

For $T\gg T_{C,N}$ the first term in Eq. (7) vanishes. On the other hand, the second term equals a constant $\frac{1}{3}S_\sigma(S_\sigma+1)$.[62] Consequently, the scattering cross section in Eq. (6) is described at $T\gg T_{C,N}$ by a one-phonon density of states weighted by the locally full symmetric electron-phonon coupling (Sec. III B). The latter favors LO(L) phonons as concluded previously[17] and confirmed by the microscopic model in Paper II.

So far we have not discussed the mechanism which is responsible for the spin dependence of the electric susceptibility in Eq. (5). A possible mechanism like in one-magnon scattering involves the coupling of the electromagnetic radiation with the spin system via spin-orbit coupling. It will be shown in Paper II that this is indeed the case as confirmed by the microscopic calculation of the resonance RS measurements in Figs. 4 and 5.

In Fig. 14(a) we show the Feynman diagram for the one-phonon one-spin RS process. The incident laser radiation of frequency ω_i creates an electron-hole pair due to the interaction $H_{\rm ehr}$. Because of the strong localization of the $4f^6$ hole in the excited intermediate state, we consider the full symmetric (Γ_1^+) electron-phonon coupling (Sec. III B) only for the $4f$

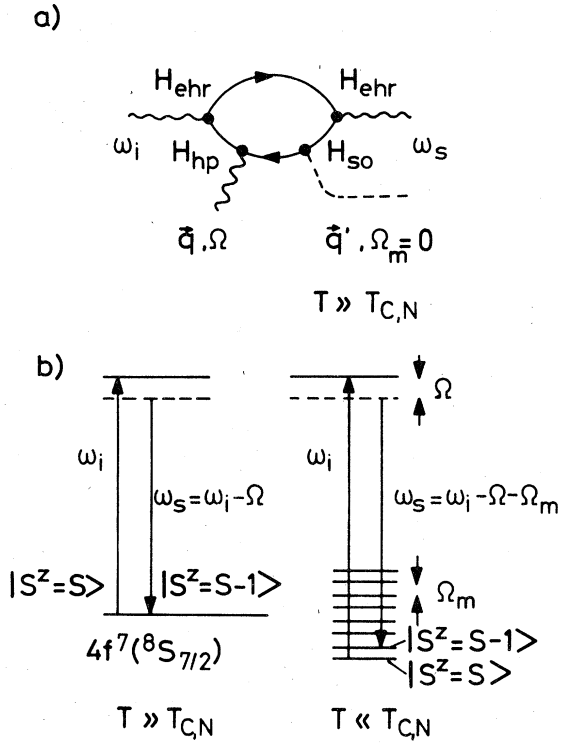

FIG. 14. (a) Feynman diagram of the one-phonon one-spin RS process of EuX in the paramagnetic phase ($T >> T_{C,N}$). ω_i (ω_s) is the frequency of the incident (scattered) photon, H_{ehr} denotes the interaction of the electromagnetic radiation with the electron-hole pair, H_{hp} is the ($4f$) hole-phonon interaction, H_{so} is the spin-orbit interaction, $\vec{q}$ ($\vec{q}'$) and Ω (Ω_m) are the momentum and frequency, respectively, of the excitation of the phonon (spin) system, with $\vec{q}' = -\vec{q}'$. (b) Electronic states involved in the RS process of Fig. 14(a) ($T >> T_{C,N}$) and for the RS process in the magnetically ordered phase ($T << T_{C,N}$).

hole as indicated by H_{hp} in Fig. 14(a). Furthermore, we consider only the spin-orbit coupling of the $4f^6$ excited hole state which amounts to $\lambda_f = 0.17$ eV.[63] The smaller spin-orbit coupling of the excited $5d$ electron is not taken into account. After recombination of the electron-hole pair a (Stokes) scattered photon of frequency $\omega_s = \omega_i - \Omega$ is emitted. The states involved in the scattering process are sketched in Fig. 14(b). The initial state in the RS for $T >> T_{C,N}$ is the eightfold degenerate $4f^7(^8S_{7/2})$ ground state of Eu^{2+}. After emitting a phonon of frequency Ω in the intermediate state, the excited electron recombines to a final state, which may differ from the initial state in the spin quantum number. Because of the degeneracy of initial and final states this gives rise to zero-frequency spin excitations $\Omega_m = 0$. However, the spin system can take up momentum $\vec{q}' = -\vec{q}$, where $\vec{q}$ is the phonon wave vector, and thus the $\vec{k}$ conservation is fulfilled.

D. Effect of magnetic order on spin-disorder-induced RS

From Fig. 14(b) follows an obvious extension of the scattering mechanism discussed above into the magnetically ordered phase ($T < T_{C,N}$). In this case the eightfold degeneracy of the ground state of the Eu^{2+} ions at $T >> T_{C,N}$ is lifted by the exchange field $H_{ex} = 2JzS/g\mu_B$, where J is the isotropic exchange coupling constant, z is the number of neighbors considered, and S is the magnitude of the spin vector. The energy separation between the $2S+1$ nondegenerate levels of different S_z values equals $\Delta = h\Omega_m M/M_s$, where M is the magnetization (sublattice magnetization) of a ferromagnet (antiferromagnet), M_s is the corresponding saturation magnetization, and Ω_m is the magnon frequency

$$\Omega_m(\vec{q}) = g\mu_B H_{ex}[1-\gamma(\vec{q})] \ ,$$

with

$$\gamma(\vec{q}) = \frac{1}{z}\sum_j \exp[i\vec{q}(\vec{r}_i - \vec{r}_j)] \ . \tag{8}$$

Consequently, we expect a transition from one-phonon zero-frequency spin excitations in the paramagnetic phase to one-phonon one-magnon scattering in the magnetically ordered phase. This is the origin of the nonlinear frequency shift of the maximum ω_0 of first-order RS of EuO and EuS in Fig. 6 upon cooling below the Curie temperature. At low temperatures $T << T_C$ the shift is expected to be $\omega_0 = \Omega_{LO}(\vec{q}_L) + \Omega_m(-\vec{q}_L)$. The values of $\Omega_m = 32$ cm^{-1} and 10 cm^{-1}, respectively, deduced from Fig. 6 for EuO and EuS are close to the values $\Omega_m(\vec{q}_L) = 44$ cm^{-1} and 8 cm^{-1} measured with neutron scattering.[64] The difference between these values can be accounted for as follows: In the magnetically ordered phase the transverse part of the second term in Eq. (7) for spin components transverse to the direction of the spontaneous magnetization (or sublattice magnetization) is the important term, while the longitudinal part vanishes at low temperature. Hence we obtain in mean-field theory for an isotropic ferromagnet[62]

$$\langle \tilde{S}_x(\vec{q})\tilde{S}_x(-\vec{q})\rangle \sim \tfrac{1}{3}S(S+1)\frac{T/T_C}{[J(0)-J(\vec{q})]/J(0)} \times \frac{n_m(\vec{q})+1}{\Omega_m(-\vec{q})}\delta(\omega-\Omega_J(\vec{q})-\Omega_m(-\vec{q})) \ , \tag{9}$$

where $n_m(\vec{q})$ is the thermal occupation factor of the magnons and $J(\vec{q}) = \sum_m J_m e^{i\vec{q}\cdot\vec{r}_m}$ is the qth Fourier component of the exchange between a spin at the origin with that located at $\vec{r}_m$. In EuX the latter term is

well approximated by considering only the nn ferromagnetic (J_1) and nnn antiferromagnetic (J_2) exchange interactions. Inserting Eq. (9) into Eq. (6) and taking into account a domain average, the scattered spectrum for $T < T_C$ is given by a weighted combined density of one-phonon and one-magnon states. As discussed in Sec. III C the locally full symmetric H_{hp} weighs heavily zone-boundary phonons, mainly LO(L) (see Paper II). On the other hand, we see from Eq.(9) that magnons with wave vectors $\vec{q} \sim 0$ are weighted most strongly. This means that the region in $\vec{q}$ space contributing substantially to the scattered spectra for $T < T_C$ is much less restricted to the sum of $\Omega_{LO}(\vec{q}_L)$ and the domain-averaged zone-boundary magnon frequency. This is why for EuO ($J_1, J_2 > 0$) the maximum at 5 K in Fig. 1 of Ref. 26 and in Fig. 6 occurs around 445 cm^{-1}, which is smaller than the sum of $\Omega_{LO}(\vec{q}_L) \simeq 414$ cm^{-1} and the zone-boundary magnon frequencies between 44 and 48 cm^{-1}.[64] However, in EuS ($J_1 > 0, J_2 < 0$) the zone-boundary magnon frequencies are much smaller than in EuO and differ strongly in magnitude for different symmetry directions, with $\Omega_m(\vec{q}_L)$ being the smallest one. The $1/\Omega_m(\vec{q})$ weighting factor in Eq. (9) favors $\Omega_m(\vec{q}_L) = 8$ cm^{-1}, which is close to the value $\Omega_m = 10$ cm^{-1} deduced from Fig. 6. In $Eu_{0.9}Gd_{0.1}S$ the Curie temperature that is roughly three times higher compared to EuS should give rise to a larger Ω_m than that of 10 cm^{-1} deduced from Fig. 6. This may be the origin of the shoulder in Fig. 11 at 7 K which extends up to 280 cm^{-1}, beyond the ω_0 peak position.

An interesting point concerns the temperature-dependence of the integrated intensity of the Raman spectra. From Eqs. (6) and (9) follows that the integrated intensity for $T << T_{C,N}$ is proportional to $n(\overline{\Omega}_m) + 1$, where $n(\overline{\Omega}_m)$ is the Bose factor and $\overline{\Omega}_m$ is an average magnon frequency, whereas for $T >> T_{C,N}$ it is proportional to $S(S+1)[n(\overline{\Omega}) + 1]$, where $\overline{\Omega}$ is an average phonon frequency. This temperature behavior was first observed by Schlegel and Wachter[10] in the case of EuS: The scattered intensity quenches below T_C, following a two-spin correlation function. This quenching below T_C can also be observed for EuO in Fig. 1 of Ref. 26. In the case of $Eu_{0.1}Sr_{0.9}S$ in Fig. 9 the nonquenching of the scattered intensity is consistent with the fact that the material does not order magnetically.

The situation is different in the case of EuTe. In the measurements reported by Güntherodt[1] and Schmutz *et al.*[65] with 6471- and 4765-Å laser lines, respectively, a strong quenching of the first-order RS is observed for temperatures below $T_N = 9.6$ K. In addition, one observes a sharp line at 113 cm^{-1} which corresponds to the scattering of LO(L) phonons induced by the antiferromagnetic spin superstructure.[1,65] However, neither the sharp line, nor the quenching of the first-order RS are observed in the spectra in Fig. 2 of Ref. 26, which have been taken with the 5145-Å laser line. These facts are indicative of a resonant effect: The excitation energy is 2.41 eV, which is only about 0.01 eV above the maximum of the E_1'' structure in the reflectivity spectra[66] [a strong resonance of the LO(Γ) scattering in the vicinity of the E_1'' peak was observed by Silberstein *et al.*[14] in the magnetic-field induced ferromagnetic phase of EuTe]. Under resonant conditions the one-spin one-phonon mechanism [see Eq. (6)] is not necessarily the most important one and higher-order perturbation terms, like the two-spin one-phonon mechanism, have to be taken into account. The fact that the sharp line at LO(L) which is associated with the one-spin one-phonon term does not show up at $T = 2$ K in Fig. 2 of Ref. 26 indicates that the two-spin one-phonon mechanism has to be considered in this case. The two-magnon one-phonon excitation has to be neglected because one would expect a stronger quenching of the intensity with decreasing temperature compared to the one-magnon one-phonon scattering process. However, the elastic scattering from the spin superstructure together with the one-magnon one-phonon excitation can explain the nonquenching of the intensity in Fig. 2 of Ref. 26. In the phenomenological treatment of this process one has to consider the following terms in the expansion of the electric susceptibility in Eq. (3):

$$\Delta\chi_{\alpha\beta} = \sum_{} R^{(2)}_{\alpha\beta,j\vec{\tau}_n} u_{j\vec{\tau}_n} S_{z,\vec{\tau}_m} S^{+}_{\vec{\tau}_m} , \quad (10)$$

with z the direction of the magnetization of one sublattice and $S^{+}_{\vec{\tau}_m} = S_x + iS_y$. The scattering cross section for this process is proportional to the product of the square of the sublattice magnetization $\langle S_z \rangle^2$ and of the two-spin correlation function. The increase of the sublattice magnetization below T_N compensates the reduction in the magnon population factor. This explains why the strong quenching of the scattering intensity observed below the magnetic ordering temperatures of EuO (Fig.8), EuS,[10] EuSe,[8] and EuTe,[1,65] far from a resonance is not observed in EuTe under resonant conditions. It is important to mention that, like in the cases of EuO and EuS discussed above, the scattered spectrum of EuTe related to Eq. (10) results from the combined, weighted density of one-magnon and one-phonon states. In EuTe the frequencies of the magnons are smaller than 4 cm^{-1}.[67] This is consistent with the fact that only minor shifts ($\lesssim 3$ cm^{-1}) are observed in Fig. 2 of Ref. 26 upon cooling from room temperature to 2 K.

IV. CONCLUSION

Although a wealth of experimental data on RS of the EuX series has been accumulated since the

pioneering work of Ray *et al.*[7] the investigations have been partly lacking the desired completeness, leading to rather controversial interpretations. This is particularly true for the symmetry-forbidden first-order RS in the paramagnetic phase of EuX.

In summarizing our experimental work presented here, which has been focused mainly on this latter point, we want to emphasize the important information that has been gained about the RS mechanism from the systematic analysis of the Raman tensor components and the measurement of their resonance enhancement. The observation of the dominant antisymmetric Γ_{15}^{+} Raman tensor component in the paramagnetic phase is the most direct prove that the phonon and spin systems are excited simultaneously and that the breakdown in $\vec{k}$-selection rule originates from the disorder of the spin system. The resonance enhancement of the Raman tensor components has given clear evidence for attributing the Γ_{15}^{+} component to the one-phonon one-spin mechanism and the Γ_{12}^{+}, Γ_{25}^{+} components to the higher-order one-phonon two-spin excitation process. The latter assignment is essentially supported by the vanishing Γ_{1}^{+} component.

For the dominant one-phonon one-spin mechanism the RS cross section is determined by the phonon and the two-spin correlation function. The scattering in the paramagnetic phase is determined by a one-phonon density of states, weighted by the electron-phonon coupling. For the latter we have proposed a locally fully symmetric 4f-hole–LO-phonon coupling, which is shown to be correct by the microscopic theory in Paper II and which is consistent with the experimentally established anion mass dependence of the first-order RS. On the other hand, the contribution of the two-spin correlation function to the RS cross section has been tested by diluting Eu^{2+}, giving rise to spin-disorder-induced RS even at low temperature.

The extension of the one-phonon one-spin scattering mechanism from the paramagnetic into the magnetically ordered phase leads to a transition from one-phonon zero-spin excitations to one-phonon one-magnon excitations, as confirmed experimentally. Under resonance conditions, as shown for the case of EuTe, the two-spin one-phonon mechanism can be of equal strength as the one-spin one-phonon excitation process. This is the reason for the nonquenching RS intensity of EuTe upon cooling below the magnetic ordering temperature, contrary to the behavior of all other EuX.

The outstanding new feature of RS in a magnetic semiconductor with respect to "normal" semiconductors is that the RS cross section depends additionally on the spin-correlation function. Hence the symmetry of the spin system determines that of the phonon system. This can give rise to spin-disorder-induced RS in the high-temperature paramagnetic phase and to magnetic "Bragg" scattering of phonons induced by spin superstructures in antiferromagnetic phases. The necessary condition for the simultaneous excitation of the spin and phonon systens is that the localized, magnetic states are initial states in RS and that the two systems are coupled, for instance, via spin-orbit coupling in the excited, intermediate state. In this sense the EuX series can be considered as a model-type class of magnetic semiconductors for the study of spin-dependent RS from phonons.

ACKNOWLEDGMENT

The authors would like to express their gratitude to M. Cardona for many fruitful discussions. The continued support of this work by M. Cardona and W. Zinn is gratefully acknowledged. We are obliged to R. Zeyher, W. Kress, A. Frey, and H. Bilz for stimulating discussions of the theoretical aspects of this work. We are indebted to R. Humphreys for pointing out to us some aspects of the experimental symmetry analysis. We would like to thank F. Canal for some help in measuring the resonance enhancement of the RS of EuSe and F. Holtzberg and K. Fischer for providing the single crystals. The authors thank H. Hirt, G. Wolff, and P. Wurster for their expert technical assistance.

---

*Present address: Coordinate Sci. Lab., Univ. of Ill. at Urbana-Champaign, Urbana, Ill. 61801.

†Institut für Feskörperforschung, KFA Jülich, 516 Jülich 1, Federal Republic of Germany.

[1]For a recent review see: G. Güntherodt, J. Magn. Magn. Mater. 11, 394 (1979).

[2]E. F. Steigmeier and G. Harbeke, Phys. Cond. Matter 12, 1 (1970).

[3]N. Suzuki and H. Kamimura, J. Phys. Soc. Jpn. 35, 985 (1973).

[4]N. Koshizuka, Y. Yokoyama, and T. Tsushima, Solid State Commun. 18, 1333 (1976).

[5]M. Iliev, E. Anastassakis, and T. Arai, Phys. Status Solidi B 86, 717 (1978).

[6]M. Iliev, G. Güntherodt, and H. Pink, Solid State Commun. 27, 863 (1978).

[7]R. K. Ray, J. C. Tsang, M. S. Dresselhaus, R. L. Aggarwal, and T. B. Reed, Phys. Lett. A 37, 129 (1971).

[8]J. C. Tsang, M. S. Dresselhaus, R. L. Aggarwal, and T. B. Reed, Phys. Rev. B 9, 984 (1974).

[9]J. C. Tsang, M. S. Dresselhaus, R. L. Aggarwal, and T. B. Reed, Phys. Rev. B 9, 997 (1974).

[10]A. Schlegel and P. Wachter, Solid State Commun. 13, 1865 (1973).

[11]V. J. Tekippe, R. P. Silberstein, M. S. Dresselhaus, and R. L. Aggarwal, Phys. Lett. A 49, 295 (1974).
[12]J. Vitins and P. Wachter, Solid State Commun. 17, 911 (1975).
[13]N. Suzuki, J. Phys. Soc. Jpn. 40, 1223 (1976).
[14]R. P. Silberstein, L. E. Schmutz, V. J. Tekippe, M. S. Dresselhaus, and R. L. Aggarwal, Solid State Commun. 18, 1173 (1976).
[15]S. A. Safran, B. Lax, and G. Dresselhaus, Solid State Commun. 19, 1217 (1976).
[16]G. Güntherodt, in *Proceedings of the 13th International Conference on the Physics of Semiconductors, Rome, 1976,* edited by F. G. Fumi (Tipografia Marves, Rome, 1976), p. 291.
[17]P. Grünberg, G. Güntherodt, A. Frey, and W. Kress, Physica (Utrecht) B 89, 225 (1977).
[18]S. A. Safran, G. Dresselhaus, M. S. Dresselhaus, and B. Lax, Physica (Utrecht) B 89, 229 (1977).
[19]J. Vitins, J. Magn. Magn. Mater. 5, 212 (1977).
[20]R. Merlin, R. Zeyher, and G. Güntherodt, Phys. Rev. Lett. 39, 1215 (1977).
[21]R. P. Silberstein, V. J. Tekippe, and M. S. Dresselhaus, Phys. Rev. B 16, 2728 (1977).
[22]S. A. Safran, G. Dresselhaus, and B. Lax, Phys. Rev. B 16, 2749 (1977).
[23]Y. Ousaka, O. Sakai, and M. Tachiki, Solid State Commun. 23, 589 (1977).
[24]O. Sakai and M. Tachiki, J. Phys. Chem. Solids 39, 269 (1978).
[25]S. A. Safran, Ph. D. thesis (MIT,1978) (unpublished).
[26]R. Merlin, R. Zeyher, and G. Güntherodt, in *Physics of Semiconductors,* edited by B. L. H. Wilson, IOP Conf. Ser. No 43 (IPPS, London, 1978), p. 145.
[27]R. Merlin, Ph. D. thesis, (Universität Stuttgart, 1978) (unpublished).
[28]J. Vitins and P. Wachter, J. Magn. Magn. Mater. 3, 161 (1976).
[29]R. Merlin, G. Güntherodt, R. Humphreys, M. Cardona, R. Suryanarayanan, and F. Holtzberg, Phys. Rev. B 17, 4951 (1978).
[30]D. C. Hamilton, Phys. Rev. 188, 1221 (1969).
[31]R. Zeyher and W. Kress, Phys. Rev. B 20, 2850 (1979) (following paper).
[32]C. F. Guerci and M. W. Shafer, J. Appl. Phys. 37, 1406 (1966); T. B. Reed and R. E. Fabey, J. Cryst. Growth 8, 337 (1971); C. Llinares, J. P. Desfours, J. P. Nadai, C. Godart, A. Percheron, and J. C. Achard, Phys. Status Solidi A 25, 185 (1974).
[33]H. Hackfort, Ph.D. thesis (Universität Kön, 1977) (unpublished).
[34]G. Güntherodt, P. Grünberg, E. Anastassakis, M. Cardona, H. Hackfort, and W. Zinn, Phys. Rev. B 16, 3504 (1977).
[35]H. Pink, Z. Anorg. Allg. Chem. 364, 248 (1969).
[36]G. Güntherodt, Phys. Cond. Matter 18, 37 (1974).
[37]The zone-center TO (182 cm^{-1}) and LO (435 cm^{-1}) phonon frequencies of EuO at 300 K have been determined from a Kramers–Kronig analysis of the reflectivity (Ref. 36). Only one set of modes has been obtained, contrary to the two-oscillator fit of Ref. 38.
[38]J. D. Axe, J. Phys. Chem. Solids 30, 1403 (1969).
[39]R. Merlin, R. Tsu, G. Güntherodt, G. Abstreiter, and M. W. Shafer, Solid State Commun. 22, 609 (1977).
[40]R. Loudon, Adv. Phys. 13, 423 (1964).
[41]R. Claus, L Merten, and J. Brandmüller, in *Springer Tracts in Modern Physics,* edited by G. Höhler (Springer, Berlin 1975), Vol. 75.
[42]W. Richter, in *Springer Tracts in Modern Physics,* edited by G. Höhler (Springer, Berlin, 1976), Vol. 78, p. 121.
[43]M. Cardona, in *Topics in Applied Physics,* edited by M. Cardona (Springer, Berlin 1975), Vol. 8, p. 9.
[44]A. Pinczuk and E. Burstein, in *Topics in Applied Physics,* edited by M. Cardona (Springer, Berlin, 1975), Vol. 8, p. 23.
[45]F. Lévy, Phys. Cond. Matter 10, 71 (1969).
[46]J. Feinleib, W. J. Scouler, J. O. Dimmock, J. Hanus, and T. B. Reed, Phys. Rev. Lett. 22, 1385 (1969).
[47]C. Llinares, E. Monteil, and G. Bordure, Solid State Commun. 13, 205 (1973).
[48]P. Streit, Phys. Cond. Matter 15, 284 (1973).
[49]K. Westerholt, B. Ghosh, K. Siratori, S. Methfessel, and T. Petzel, Physica (Utrecht) B+C 86-88, 740 (1977).
[50]H. Maletta, W. Felsch, and J. L. Tholence, J. Magn. Magn. Mater. (to be published).
[51]T. Penney, M. W. Shafer, and J. B. Torrance, Phys. Rev. B 5, 3669 (1972).
[52]T. R. McGuire and F. Holtzberg, in *Proceedings of the 17th Conference on Magnetism and Magnetic Materials, Chicago, 1971,* edited by C. D. Graham, Jr. and J. J. Rhyne, AIP Conf. Proc. No. 5 (AIP, New York, 1972), p. 855.
[53]K. H. Rieder, B. A. Weinstein, M. Cardona, and H. Bilz, Phys. Rev. B 8, 4780 (1973). K. H. Rieder, R. Migoni, and B. Renker, Phys. Rev. B 12, 3374 (1975).
[54]M. L. Williams and J. Smit, Solid State Commun. 8, 2009 (1970).
[55]*CRC Handbook of Chemistry and Physics* (Chemical Rubber, Cleveland, 1975), p. F-209.
[56]M. J. Freiser, F. Holtzberg, S. Methfessel, G. D. Pettit, M. W. Shafer, and J. C. Suits, Helv. Phys. Acta 41, 832 (1968).
[57]P. A. Fleury and R. Loudon, Phys. Rev. 166, 514 (1968).
[58]I. Dabrowski, P. Grünberg, and J. A. Koningstein, J. Chem. Phys. 56, 1264 (1972).
[59]T. G. Spiro and T. C. Strekas, Proc. Nat. Acad. Sci. U.S.A. 69, 2622 (1972).
[60]E. Mulazzi and N. Terzi, Solid State Commun. 18, 721 (1976).
[61]T. Moriya, J. Phys. Soc. Jpn. 23, 490 (1967).
[62]W. Marshall and R. D. Lowde, Rep. Progr. Phys. 31, 705 (1971).
[63]T. Kasuya, CRC Rev. Solid State Sci. 3, 131 (1972).
[64]L. Passell, O. W. Dietrich, and J. Als-Nielsen, in *Proceedings of the 17th Conference on Magnetism and Magnetic Materials, 1971, Chicago,* edited by C. D. Graham, Jr. and J. J. Rhyne, AIP Conf. Ser. No. 5 (AIP, New York, 1971), p. 1251.
[65]L. E. Schmutz, G. Dresselhaus, and M. S. Dresselhaus, J. Magn. Magn. Mater. 11, 412 (1979).
[66]J. Feinleib and C. R. Pidgeon, Phys. Rev. Lett. 23, 1391 (1969).
[67]S. Maekawa, J. Phys. Soc. Jpn. 34, 1477 (1973).